CFD Letters

Journal homepage:
https://semarakilmu.com.my/journals/index.php/CFD_Letters/index
ISSN: 2180-1363

Numerical Study on the Effect of Four-Lobe Swirl Generator and Its Transition Parts on Thermal Performance Enhancement and Fluid Flow

Farag A. Diabis[1,2], Abd Rahim Abu Talib[1,*], Norkhairunnisa Mazlan[1], Eris Elianddy Supeni[3]

[1] Aerodynamic, Heat Transfer and Propulsion Group, Department of Aerospace Engineering, Faculty of Engineering, Universiti Putra Malaysia, 43400 Serdang, Selangor, Malaysia
[2] The General Electricity Company of Libya (GECOL), Tripoli, Libya
[3] Department of Mechanical and Manufacturing Engineering, Faculty of Engineering, Universiti Putra Malaysia, 43400 Serdang, Selangor, Malaysia

ARTICLE INFO

Article history:
Received 12 December 2024
Received in revised form 17 January 2025
Accepted 15 February 2025
Available online 30 April 2025

Keywords:
Heat transfer; lobed swirl device; twisted angle; transition multipliers; variable helix

ABSTRACT

Improving heat transfer in the field of thermal application is the targeted outcome of many researchers. The flow within smooth channels could not be mixed properly. Therefore, swirl flow techniques are taken into consideration because of their capability to promote the heat exchanger's thermal efficiency by changing the flow's direction and creating a fluctuating flow between the channel's wall and core. The primary challenge that researchers frequently encounter with swirl flow techniques is the increased pressure loss. One of the most notable recent advancements is the lobed swirl generator, which achieves substantial swirl intensity with manageable pressure loss. Consequently, this study aims to explore and gain a deeper understanding of the thermal characteristics of the lobed swirl generator under various performance parameters. Consequently, the impact of a four-lobed swirl generator under a different twisted angle of ($90 \leq \theta \leq 450$) and its transition part at essential parameters of transition multipliers ($0.25 \leq n \leq 0.75$) and variable helix ($0.5 \leq t \leq 1.5$) have been examined. The working fluid is water at the Reynolds number varies from 30,000 to 55,000 is conducted. The applicable shear-stress transport (*SST*) k-ω model has been adopted to model the turbulence swirling flow. According to the obtained results, the lobed swirl generator at (θ =360) and beta transition of (n = 0.5 mm) and (t =1 mm), the heat transfer and pressure loss increase compared with plain tube by 28.78 % and 17.35 %, respectively. By reducing the transition multipliers value to (n = 0.25 mm), a slight increase in heat transfer and pressure loss in the percentage by 40.32 % and 17.89 %, respectively are observed. The outcome demonstrated that lobed swirls could generate a centrifugal force under different conditions, which is the main significant character behind the heat transfer improvement.

1. Introduction

The efficiency of heat exchangers is a vital step to overcoming the challenges of the energy crisis as mentioned in the previous study by Jiang *et al.,* [1]. The limited availability of natural fuel supplies, growing energy prices, and environmental concerns drive enterprises to improve the energy

* *Corresponding author.*
E-mail address: abdrahim@upm.edu.my (Abd Rahim Abu Talib)

https://doi.org/10.37934/cfdl.17.10.120148

efficiency of thermal application systems. Various techniques have been presented in the past years to improve heat transfer (HT), as studied by the literature [2,3]. Passive and active methods are classified as essential techniques in many thermal applications according to Mousavi Ajarostaghi *et al.,* [4]. The heat transfer enhancement accompanied by maintaining the pressure drop at the practical value is considered the main target of this study. The mechanism of heat transfer improvement can also be divided into three categories:

i. the effects of rough surface led to mixing between the adjacent fluid on the wall and the mainstream
ii. the influence of the impingement jet directly results in the thermal boundary layer decreasing
iii. the impact of tube rotating engendered secondary or swirl flow, as conducted by Tang *et al.,* [5].

The four-lobe swirl generator (4-LSG) can be utilized in a wide range of industries, including power generation, aerospace, automotive, HVAC, and chemical processing are taken from Li *et al.,* [6]. The lobed swirl can enhance heat transfer, improve mixing, and induce turbulence making it an essential tool for optimizing thermal systems, reducing energy consumption, and ensuring reliable operation in in various industries. Applying a swirl generator in a solar power system can enhance heat transfer in thermal energy harvesting and storage systems, as conducted by Rashidi *et al.,* [7]. It is found that the lobed swirl is used in marine boilers to improve their heat exchanger efficiency, as confirmed by Ariyaratne *et al.,* [8]. Due to its advantage of improving the thermal performance of smooth channels without changing their geometrical cross-section, the implementation of lobed swirl generators in heat exchangers is highly recommended. Improved heat transfer in evaporator and condenser units allows for more efficient cooling and reduced energy consumption. Therefore, A compact refrigeration system with four-lobe swirl generators in the refrigerant lines can enhance heat transfer while reducing system size. The benefit of the swirl flow is induced tangential velocity adjacent to the wall, and axial velocity concentrated on the core, causing secondary flow and vortex motion based on the literature examined by Brar *et al.,* [9] and Stroh *et al.,* [10], which are considered the main reason for heat transfer enhancement. From the mechanisation perspective of the swirl flow, significant attention has been paid to many studies to innovate the appropriate thermal applications such as; corrugated channel, twisted tape, conical wire, radial blades, conical porous honeycomb, internal spirals, backwards-facing channels, helical ribs based on the literature examined [11-19]. The characteristic of swirl flow is represented in its ability to improve heat transfer based on a review of Bezaatpour *et al.,* [20]. The primary features of the swirl flow are decreased thermal boundary layer gradient, development of secondary flow, and mixing of the flow between the core and the wall as taken from the preceding look at Shlash *et al.,* [21].

The tangential and axial velocities induced from the swirl flow downstream are responsible for these characteristics as illustrated by Wang *et al.,* [22]. The most critical factors that improved the heat transfer generated by swirl flow are considered to be the centrifugal effect, the increase of the flow adjacent to the wall (tangential velocity), and the increase of the level of turbulent flow as performed by Gorelikov *et al.,* [23]. Three indispensable types listed below are considered to describe the characteristics of swirl flow:

i. the fluid flow receives tangential velocity and is inducted as a rotating form through the pipe
ii. the swirl flow is generated due to the effect of certain angles (blades) placed at the entrance of the tube
iii. due to the curvature shape, the flow formed as tangential and induced through the tube as a swirl flow as indicated from the previous observe as discussed in earlier study by Gorelikov *et al.,* [23].

The improvement of heat transfer, simple fabrication and self-supporting are considered the main advantages of spiral tubes as undertaken in Shahsavar *et al.,* [24]. Helical pipe characteristics in the field of heat transfer are described as follows:

i. the feature of its curvature cross-section caused secondary and velocity flow within the tube downstream,
ii. generated mixing flow between the core and the wall, it became obtained from Omidi *et al.,* [25].

Due to its advantages of simple construction, low cost, and accessible integration, a lobed swirl generator is highly recommended to increase the thermal performance of heat exchangers, as observed by Yan *et al.,* [26]. Many researchers have presented numerous innovations in thermal performance applications to promote heat transfer and address the pressure drop penalty Based on the results of the previous study by Waware *et al.,* [27] and Kore *et al.,* [28]. Experimentally and numerically, the effect of twisted angles from 90º-360º and different lengths from 0.2 to 0.4 m using a three-lobe swirl generator has been investigated by Jafari *et al*., [29]. The result presented the highest heat transfer and thermal performance of 1.74 and 1.55, respectively, under the length of 400 mm and the twisted angle of 360º. On the other hand, at a fixed length of (0.4 m) and the same different crooked angles, the four-lobe swirl generator was also examined experimentally and numerically by Jafari *et al*., [30]. Compared with the three-lobe, the result showed a considerably improved heat transfer and thermal performance by 1.87 to 1.65, respectively. To examine the effectiveness of lobe number, Jafari *et al*., [31] studied the impact of a five-lobe swirl generator under the exact angles (90º, 180º, 270º and 360º) and the same length (0.2, 0.3 and 0.4 m) on heat transfer and thermal performance. The result presented an improvement in heat transfer and thermal performance by a factor of 1.74 and 1.55, respectively, associated with the angle of 360º. A comparison between the recent studies is listed in Table 1.

A numerical simulation of the impact of a helical coil on heat transmission and fraction factor was performed by Omidi *et al*., [25]. The geometrical cross-section of the helical coil under different lobe numbers and flow regimes ranging from 1,300 to 2,500 (laminar flow) has been investigated. The result proved that the increased lobed number led to improved thermal performance. A comparison between twisted oval tube and tri-lobe in order to investigate their impact on heat transfer and fluid field at turbulent flow ranging between Reynolds number of 8,000 to 21,000 numerically and experimentally performed by Tang *et al*., [5]. The study was carried out under several parameters of twisted pitch and direction, cross suction, and lobe number. The study proved that the tri-lobe geometrical cross-section significantly improves heat transfer by 5.4% compared to the oval tube, with an increasing fraction factor of 8.4%. The result also exhibited that the lobe cross section applied potentially affects heat transfer enhancement with increased fraction factor compared with a plane tube. The effect of the multi-lobed swirl generator of 3, 4, 5, 6, 8, 9 and 10-lobe are numerically examined by Yan *et al*., [26]. The study also focused on the pitch-to-diameter (*P/D*) effect as the

influential factor on pressure drop and the rate of swirl decay. The study was performed at turbulent flow ranging between 4,583 and 35,000. Among all parameters studied, the swirl generator in terms of four-lobed indicated the optimum value of swirl effectiveness at the (*P/D* = 8) associated with quite an increase in the ratio of a fraction factor value.

Table 1
Summary of recent studies exhibiting the thermal performance improvement of lobed swirl number

Ref.	Physical model	Approach	Working fluid	Flow regime	Observation
[30]	4-LSG	Experimental & numerical	water	6,000 ≤ *Re* ≤ 30,000	4-LSG improved HT and PEC by factors 1.87 and 1.65, respectively.
[31]	5-lobe	Experimental	water	6,000 ≤ *Re* ≤ 30,000	*Nu*&PEC enhanced to 1.84 and 1.65, respectively.
[32]	4-LSG	Numerical	SiO_2, Al_2O_3, and CuO- nanofluid	15,000 ≤ *Re* ≤ 35,000	An improvement in HT and PEC to 1.87 and 1.67, respectively, with SiO_2-Nanofluid.
[33]	Coil tube (3, 4, & 5 lobes)	Numerical	water	15,000 ≤ *Re* ≤ 40,000	Thermal efficiency of 19.16%. obtain Re of 35,000
[34]	Twisted tri- & oval tubes	Numerical	supercritical water (SCW)	8,000 ≤ *Re* ≤ 20,000	Nu of tri-lobed at 53% and 41%, respectively observed
[35]	Four triangular lobes	Experimental	Water–ethylene glycol mixtures	12,000 ≤ *Re* ≤ 27,000	Improve heat transfer and pressure drop up to 75% and 55%, respectively.
[36]	Tri-lobe tube with twisted tape	Numerical	water	5,000 ≤ *Re* ≤ 20,000	Thermal performance improvement is inversely proportional to the growth of the *Re*. A higher *Re* causes a greater *Nu* at the same baffle size ratio.

Ariyaratne *et al.,* [37] presented studying on the improvement of lobed swirl efficiency for the transportation of particle-bearing liquids by designing the transition part before and after the swirl device itself. The study showed surprising benefits in the impact of the transition parts mounted before and after the swirl device. Increase the swirling overall within the entry transition part and reduce the swirling decay caused due to the exit transition part, considered the main feature of transition parts implementation. The study proved that the effectiveness of transition parts is highly dependent on several parameters, such as Alpha transition (α), beta transition (β), transition multiplier (n) and variable helix (t). Reducing the overall pressure is a vital step to improve the effectiveness of the lobed swirl generator as taken from Bezaatpour *et al.,* [38]. Therefore, many studies on the effect of lobed swirl with its transition part have been presented to develop a new lobed swirl generator technique. A comprehensive study on the impact of different lobed suctions at laminar flow ranging from 500 to 2,500 on thermal performance and fluid flow has been investigated by Rezaei *et al.,* [39] The study is conducted at several geometrical parameters such as; lobed model, twisted angle and lobed number. In comparing with a smooth channel, the result revealed that the spiral tubes associated with a lobed cross-section are not affection in Reynolds number greater than 1,000 and a twisted angle greater than zero. Hamdan [40] presented a study of the effect of swirl flow under laminar flow. The outcome proved that the inlet of swirl flow and the range of Reynolds number has a significant impact on swirl decay. Spiral coils under laminar and turbulent flow regimes have

been studied by Patil [41]. The study confirmed that the friction factor increases by the value of 24%, while the Nusselt number (*Nu*) 20%. In comparison with turbulent flow, the study revealed that the performance of spiral tubes with laminar flow is greater than turbulent flow. Li *et al*., [42] conducted a numerical study to investigate the four-lobe swirl generator under different lengths (0.6 and 0.4 m) on the flow field's effect and the lobed swirl's effectiveness. The result proved that the four-lobe swirl generator at a short length presents considerable improvement in swirl effectiveness compared with the long one. The study confirmed that the four-lobe swirl generator associated with short length is more efficient with a high *Re*.

From the literature review and other comprehensive studies, it can be proved that applying a lobe swirl generator in the field of thermal application can improve thermal performance with a practical level of pressure loss. However, there is no numerical study performed on a four-lobe swirl generator under different angles, and the effective parameters of transition parts such as beta transition (β), transition multipliers factor (*n*) variable helix (*t*) on the heat transfer and fluid flow. Although prior research has demonstrated the effectiveness of swirl flow techniques, the influence of lobed number, lobed twisted angle (ϑ), transition multiplier (*n*) and transition variable helix (t) on thermal efficiency and flow dynamics has not been adequately addressed. Also, the interplay between heat transfer enhancement and pressure loss in advanced swirl generators has yet to be comprehensively analysed under varying Reynolds numbers. The most significant recent development is the lobed swirl generator, which produces considerable swirl intensity with an applicable pressure loss. Therefore, the motivation behind this study is to investigate and acquire a deeper understanding of the lobed swirl generator's thermal characteristics under various effective parameters. With its ability to enhance thermal performance while reducing pressure loss, the four-lobe swirl generator is considered promising for heat exchangers, HVAC systems, and chemical processing applications. This study seeks to explore its potential under various operational conditions. Maintaining the pressure drop at an acceptable level in swirl flow applications is still challenging when the heat transfer enhancement has the target outcome. Therefore, additional techniques are still required to overcome the pressure drop penalty. Consequently, the main objectives of this study are:

i. to study the effect of a lobed swirl generator under a different angle and constant of length, transition multiplier and transition variable helix on thermal performance
ii. to investigate the effect of the beta transition (β) part under different multipliers (*n*) on heat transfer and pressure drop
iii. to examine also the effect of the beta transition (β) part at several variable helices (*t*) on heat transfer enhancement.

2. Methodology

2.1 Physical Model

2.1.1 Scope of parameters

The current study's scope involves investigating the properties of swirl flow caused by a four-lobed swirl generator and its appealing transition parts across a smooth channel. This study was performed under different geometrical parameters utilising water as a working fluid. The research performed the lobed swirl generator at different twisted angles to evaluate its impact on heat transfer under varied swirl flow. On thermal performance characteristics Jafari *et al.,* [30] investigated a 4-lobed swirl generator under different twisted angles of (90^o to 360^o), and Li *et al.,* [42] performed the same swirl on the field of Clean-In-Place under the twisted angle of (360^o and 540^o). Consequently, the current study aims to analyse the 4-lobed swirl generator with its appealing

transition parts at the twisted from (90^o to 540^o), to explore the impact of the lobed swirl generator on thermal performance. According to the twisted length of a lobed swirl generator, many studies proved that the effectiveness of a lobed swirl generator can be obtained at a twisted length of 0.4 m, as undertaken in the previous study by Li *et al.,* [42] and Jafari *et al.,* [43] and Pitch to a diameter of 8, as mentioned in the studies of Yan *et al.,* [26] and Ganeshalingam [44]. Therefore, the current studies adopted this value as the optimum design. Regarding the lobed number, the adoption of 4-lobed is based on the studies of Jafari *et al.,* [30,31] and Hamdan [40] and the comparison between a different lobed number (3, 4, 5, 6, 8, 9, 10 lobed) conducted by Yan *et al.,* [26] and a comparison study performed by Ganeshalingam [44], which all proved that the 4-lobed swirl generators were more efficient than all of the lobed numbers investigated. The following advantages motivate the use of water as a working fluid, as discovered in the previous study by Qazi [45]:

i. suitable heat transfer fluid
ii. low viscosity
iii. high thermal capacity
iv. cheaper to use.

A comparison between beta transition (β) and alpha transition (α) was undertaken by Ariyaratne [46]. The study revealed that the β-transition is more efficient than α- transition by the value of 5%; as a result, β-transition was adopted in the present study. The transition parts can reduce the pressure loss, improve the overall swirl intensity, and reduce the swirl decay, as stated Ariyaratne *et al.,* [37]. Therefore, the same length of 0.1 m has been employed in the current study. There are two practical factors related to the transition parts. The transition multiplier (n) controls the intermediate area of transition parts at the n-value. The other parameter, known as a variable helix (t), leads to a decrease or increase in the transition helix as desired. Therefore, examining transition parts at different transition multipliers of (n = 0.25, 0.5, 0.75 mm) and the variable helix (t = 0.5, 1, 1.5 mm) was also the target outcome behind this study. Li *et al.,* [42] proved that the lobed swirl generator is more efficient with a high Reynolds number; as a result, a Reynolds number between 15,000 and 55,000 was used in the present study. Applicable shear-stress transport (SST) k-ω model was used to model the turbulence swirling flow and the pressure adverse.

2.1.2 Four-lobe swirl device

The Reference Geometry Plane technique and Left Boss/Base feature of SolidWorks software were used to plot the geometrical cross-section in the current study. Based on the lobed swirl generator suggested in the literature, the lobed swirl device at the length of 0.2 m and the equivalent diameter of 0.5 m was adopted as the optimum design. The swirl flow induced by the lobed swirl generator gains tangential velocity noticeable adjacent to the wall and axial velocity concentrated at the core from Jafari *et al.,* [30]. To evaluate the lobe swirl device, three essential radii should be taken into consideration, tube radius (R), lobe radius (r_{lobe}) and the radius of the polygon area (R_{sc}), as shown in Figure 1. In addition, the angle (θ) which has a vital step to create lobe curvature takes place.

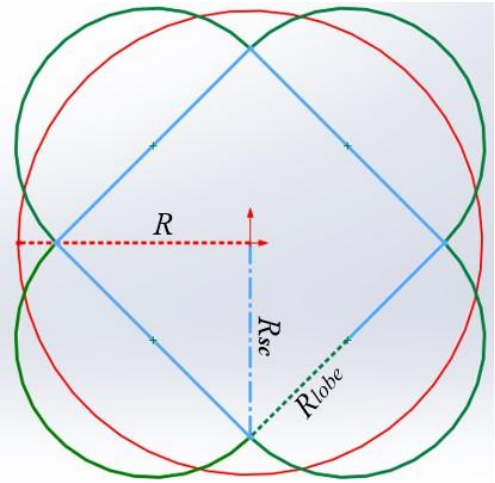

Fig. 1. Primary radii of lobe swirl device

The lobe swirl device was constructed by dividing and allocating parallel planes, as seen in Figure 2. To avoid the steeper and ensure the constant twisted angle across the geometric cross-section, the distance between every two adjacent planes at 10 mm (x/L = 0.05) is also taken into consideration. As a result, each adjacent plane would have an angle of 4.5º, 9º, 13.5º, 18º and 13.5º based on the adopted swirl angle of 90º, 180º, 270º, 360º and 450º respectively as indicated from the previous observation as discussed in earlier study by Li [47]. For all geometrical cross sections studied, the lobe radius (r_{lobe}) and the polygon radius (R_{cs}) were measured using Eq. (1) and Eq. (2).

$$r_{lobe} = \sqrt{\frac{2\pi \tan\left(\frac{360}{8}\right)R^2}{8+4\pi+\tan\left(\frac{360}{8}\right)}} \tag{1}$$

$$R_{CS} = \frac{r_{lobe}}{\sin\left(\frac{360}{8}\right)} \tag{2}$$

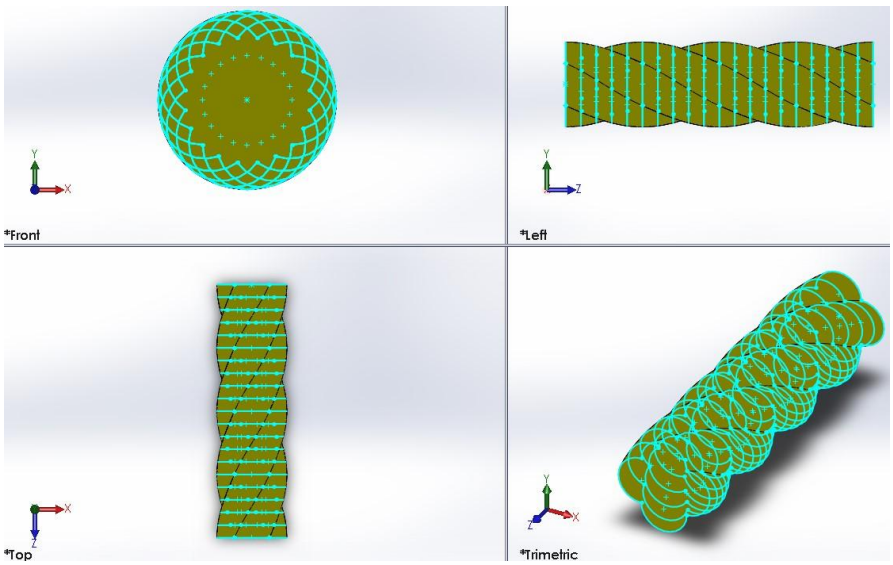

Fig. 2. Lobe swirl device under 21 planes from different sides at (θ = 360º

The hydraulic diameter, cross-sectional area, and perimeter using Eq. (3), Eq. (4) and Eq. (5) are evaluated as follows:

The four lobes area (A_{4L}) = the polygon area at the centre (A_p) + the area of four segments on the sides (A_{4s}). Therefore:

$$A_{4L} = \frac{r^2{}_{lobe}}{tan\left(\frac{360}{2}\right)} \times n + \frac{\pi r_{lobe}^2}{2} \times n \tag{3}$$

$$P_{4L} = n \times \frac{2\pi r_{lobe}}{2} \tag{4}$$

$$D_{h_{4L}} = \frac{4A_{4L}}{P_{4L}} D_{h_{4L}} = \frac{4A_{4L}}{P_{4L}} \tag{5}$$

2.1.3 Transition part

The transition part is considered an important essential parameter to increase the effectiveness of the lobed swirl intensity and decrease the pressure losses of swirl flow downstream. Consequently, saving energy and cost as conducted by a previous study by Esfe *et al.,* [36]. According to previous research, a sudden change in lobe cross-section during fluid flow increases pressure losses [37]. As a result, the gradual development of the transition region from a circular cross-section to a lobe shape and vice versa led to a reduction in pressure loss and improvement in the efficacy of lobed swirl.

To create the cross-section of the transition part, the Reference Geometry Plane and Lofted Boss/Base features of the SolidWork-2015 software were used. The transition twist was calculated using Eq. (6). based on the equivalent diameter (d_e) and pitch to diameter (*P:D*). Therefore, Eq. (7) was used to determine the optimum transmission parts length. To ensure the gradual change of the transition part from a circle shape to a lobe and vice versa, the curvature of the cross-section was turned quarter (1/4) or from increment angle (45º) no lobe to (90º) at fully developed. To simplify the calculation of variables (*R* & *y*), two crucial variables (*f&f1*) based on a trigonometric function have been introduced using Eq. (8) and Eq. (9). The core radius (*R*) was calculated using Eq. (10). By introducing the variable (*y*) using Eq. (11), it was simple to keep the growth of the lobe area constant at each stage. The intermediate area development at each stage (LA_i) and fully developed (LA_{FD}) were calculated using Eq. (12) and Eq. (13). To avoid discontinuity in the area during the development of the transition part at the start and the end regions, the cosine function has been adopted using Eq. (14).

$$twist(deg\,r\,ee/m) = \frac{360}{(P{:}D_{ratio}) \times de} \tag{6}$$

$$L_t = \frac{1000mm}{Twisted(deg\,ree/m)} \times 90° \tag{7}$$

$$f = \left(\gamma - \frac{1}{2} sin\,2\,\gamma\right) \tag{8}$$

$$f_1 = \frac{1}{2}\left[1 - \frac{1}{1 - tan\,\gamma}\right] \tag{9}$$

$$R = R_1 \sqrt{\frac{\pi}{4f + 4ff_1 - 4\sqrt{2}ff_1 + 2}} \tag{10}$$

$$y = f_1 \times R \tag{11}$$

$$LA_i = 4r_{lobe}^2 - R^2(\pi - 2) \tag{12}$$

$$LA_{FD} = r_{lobe}^2(4 + 2\pi) - \pi R_{CS}^2 \tag{13}$$

2.1.3.1 Alpha and beta transitions

From the perspective of lobed area development, there are two vital parameters: Alpha transition (α) and beta transition (β). The *α* represents the ratio between the area at the intermediate stage to the fully developed region, which can be evaluated using Eq. (14). Regarding β, it is dependent on the relation between the core area and the intermediate and fully developed regions. Eq. (15) was used to evaluate beta transition. Ariyaratne *et al.,* [37] proved that the β presented an improvement in swirl effectiveness of 5% more than the *α*. Therefore, the β has been adopted in the current study.

$$\alpha = \frac{LA_i}{LA_{FD}} \tag{14}$$

$$\beta = \frac{\frac{LA_i}{\pi R^2 - LA_i}}{\frac{LA_{FD}}{\pi R^2 - LA_{FD}}} \tag{15}$$

2.1.3.2 Transition multiplier (n)

The transition multiplier is the parameter used to control the intermediate area of the transition section in each stage at the variation of the (*n*) value given. The *n* is the leading factor that affects the lobe area development, especially at the start and the end of the transition part region. Ariyaratne *et al.,* [37] compared the alpha transition (α) and beta transition (β) under different values on the effect of lobed area development. The study demonstrated that the β presented a 50% point close to the start, more incredible than the *α* for all the variables studied. The result implies that the β has remarkable effects on the development of the lobe area. Eq. (16) and Eq. (17) are used to introduce the effect of the transition multiplier.

$$\alpha = \left[\frac{AL_i}{AL_{FD}}\right]^n \tag{16}$$

$$\beta = \left[\frac{\frac{LA_i}{\pi R^2 - AL_i}}{\frac{LA_{FD}}{\pi R^2 - LA_{FD}}}\right]^n \tag{17}$$

2.1.3.3 Variable helix (t)

The variable helix (*t*) is considered the critical parameter that directly impacts the twisting shape during the development of the transition part. According to the twisting changing with respect to the length, there are two helix types. Geodesic, if the helix developed stationary over the transition part. In other meaning, the power law (*t* =1) [37]. The second type is the brachistochrone helix, which was investigated by Raylor [48]. The power law in the brachistochrone helix method should be less or greater than one. The increase or decrease of the helix along the transition part depended on the value of the *t* given. In the case of a *t* set greater than one, the helix formed faster near the exit of

the transition part. In terms of the *t* value fixed smaller than one, the helix becomes faster at the entry of the transition part. Eq. (18) was adopted to determine the twisting of the transition part at the desired value of a *t*. The transition part from different sides is demonstrated in Figure 3.

$$Twist[0,90°] = \left(\frac{x}{L}\right)^{t} \times 90° \times Twistedd(diraction) \tag{18}$$

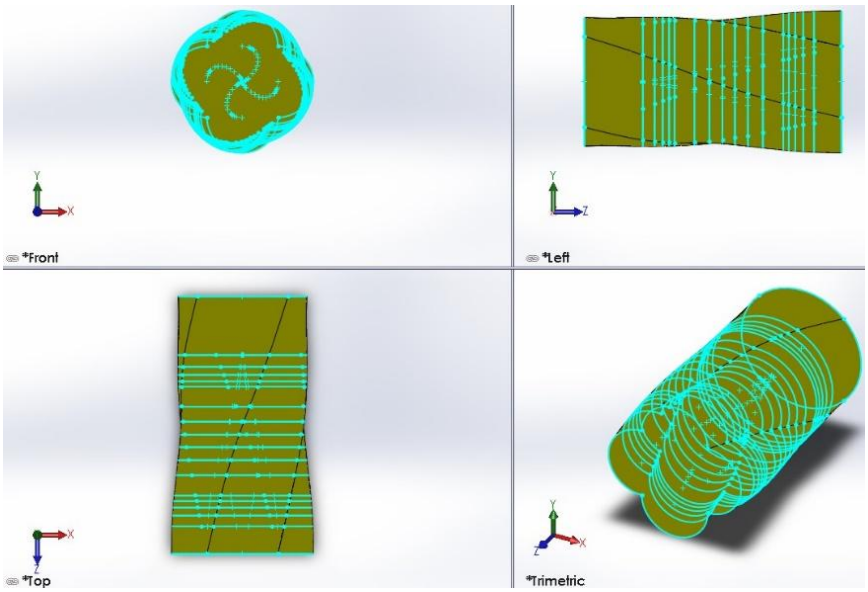

Fig. 3. Transition part under 18 planes from different sides at (θ =360º)

2.2 Numerical Approach

2.2.1 Computational domain

The 3-D solid domain system was constructed using SolidWork-2015. As depicted in Figure. 4, it can categorise the solid domain into different essential parts. According to a given *Re* and the tube diameter of 0.5 m using Eq. (19), the entry section was extended enough to ensure the fully developed turbulent flow. As practical factors, the transition parts and the lobed swirl generator lengths were adopted at 0.1 and 0.2 m, respectively. The testing copper tube at 1 m was subjected to constant heat flux. The working fluid in a current numerical study is water, and the turbulent flow is generated at the *Re* range of 3,000 to 55,000 due to the effectiveness of a short-lobed swirl generator at a high *Re* as mentioned by Li [47]. The current numerical study was performed to examine the effect of the lobe swirl generator at different helical twisted angles from 90º to 450º on the flow field and thermal performance.

$$L_e = 4.4D \times (\mathrm{Re})^{1/6} \tag{19}$$

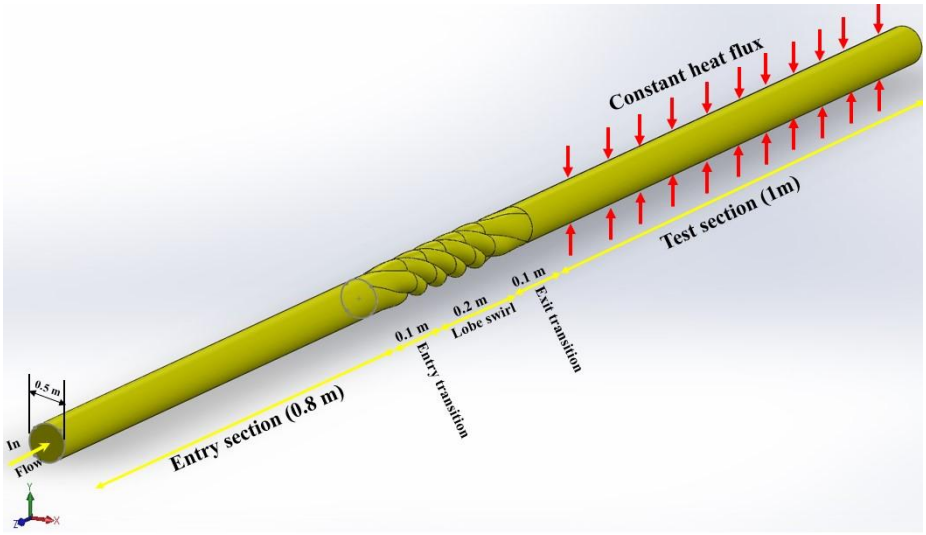

Fig. 4. The lobed swirl generator in 3-D mode as a solid domain

2.2.2 Meshing

The Integrated Computer Engineering and Manufacturing (ICEM-CFD) Ansys, 2020 R2 was utilised to mesh the geometry using hexahedral cells. Using structured mesh and hexahedral cells enables the solver to run faster and decrease the numerical diffusion. In the case of complex geometry such as lobed swirl, the structured mesh is more efficient than the unstructured mesh because it facilitates the need to refine the mesh as conducted in the study by Li *et al.,* [49]. The geometrical cross-section of the four-lobe swirl generator contains many sharp angles making the application extremely complex. Consequently, ICEM-CFD software is used due to its ability to deal with complex geometries and its top-down Blocking feature. Regarding the twisted angle of the geometrical cross-section, the block was split into different distances, then created and rotated the O-grid blocks as shown in Figure 5 (a) to 5(c). The figures illustrate the surface mesh around the associated block generated at different lobed swirl angles. The steps for generating the mesh using ICEM CFD software are listed below:

i. The centre point at the plane corners is established using the (centre of 3 points/Arc) option.
ii. The parts of the boundary condition are generated by selecting the entities feature, and the fluid body is created using the location option.
iii. All the appropriate visible objectives are selected, and the block is subdivided by utilizing the recommended point and edge selections.
iv. An O-grid block is constructed by selecting both the block and faces options.
v. The vertices, centre points, rotational angles, and vectors are selected, and the rotate vertices technique is applied to change their positions.
vi. The block is subdivided into several parts based on the twisted angles, after which the rotate option is selected to create the O-grid blocks.
vii. The blocking association method is chosen to join the vertex to the point and the edge to the curve.
viii. The Pri-Mesh Parms option is applied to generate the mesh.
ix. The mesh quality is checked using the Pre-mesh quality histogram function, ensuring the angle is more than 18º.
x. The mesh is smoothed if necessary.
xi. The output mesh is specified, and the solver is determined.

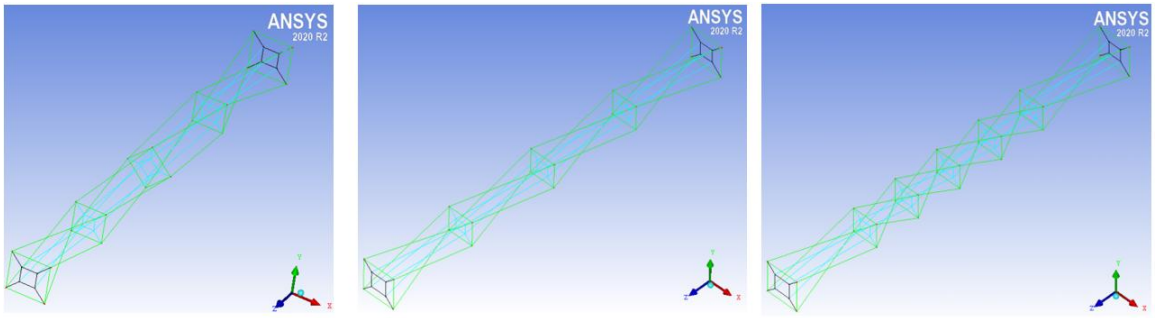

Fig. 5. O-grid around different lobed swirl angles (a) 90° (b) 180° (c) 360°

The surface mesh created around the related block at various lobed swirl angles is shown in Figure 6(a) to 6(c).

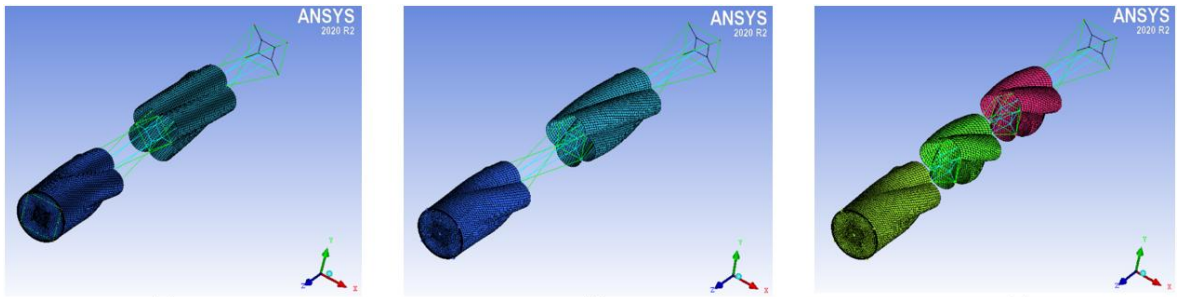

Fig. 6. Generated surface mesh around the associated block at different lobed swirl angles (a) 90° (b) 180° (c) 360°

The advantage of the SST *k-ω* model is modifies asymmetric diffusion ingredients and improves the turbulent viscosity to accurately predict the fluid separation caused by a negative pressure gradient [29]. The flow is turbulent, single-phase, and incompressible. Twisted tri-lobed and oval tubes have been studied by Tang *et al*., [5]. The study verified the solver's ability to predict the reliability and validation of the outcome by comparing the experimental and numerical results under different turbulent models such as the SST *k-ω* model, Standard *k-ω* model, Reliable *k-ε* model, RNG *k-ε* model and RSM model. Among all modelling investigated, SST *k-ω* presented considerably corresponded between the experimental and numerical results. To ensure the meshed of the viscous sublayer during the employed SST *k-ω* model, the cell size close to the wall, similar to the dimensionless distance wall Y+, should be smaller than 4 as mentioned in the previous study by Oneissi *et al.,* [50]. Therefore, the SST *k-ω* model was adopted in a current numerical study. The governing equation (Navier-Stokes Equation) is considered to predict the swirl flow generated by lobed swirl devices. The equations of mass, momentum and energy are involved in the present investigation as follows:

Continuity equation:

$$\frac{\partial}{\partial x_i}\left(u_i\right)=0 \tag{20}$$

Momentum equation:

$$\frac{\partial\left(\rho u_i u_j\right)}{\partial x_i}=-\frac{\partial p}{\partial x_i}+\frac{\partial}{\partial x_j}\left[\mu\left(\frac{\partial u_i}{\partial x_j}+\frac{\partial u_j}{\partial x_i}-\frac{2}{3}\delta_{ij}\frac{\partial u_i}{\partial x_j}\right)\right]+\frac{\partial}{\partial x_j}\left(-\rho\overline{u_i' u_j'}\right) \tag{21}$$

Energy equation:

$$\frac{\partial}{\partial x_i}\left(u_i\left(E\rho+P\right)\right)=\frac{\partial}{\partial x_j}\left[\left(\lambda+\frac{Cpu_t}{\mathrm{Pr}_t}\right)\frac{\partial T}{\partial x_j}+u_i\left(\tau_{ij}\right)_{eff}\right] \tag{22}$$

where E is the overall energy and $(\tau_{ij})_{eff}$ is the deviation of the stress tensor, which are evaluated as follows:

$$E=CpT-\left(P/\rho\right)+\frac{u^2}{2} \tag{23}$$

$$\left(\tau\right)_{eff}=\left[\mu_{eff}\left(\frac{\partial u_j}{\partial x_i}+\frac{\partial u_i}{\partial x_j}\right)-\frac{2}{3}\mu_{eff}\frac{\partial u_i}{\partial x_j}\delta_{ij}\right] \tag{24}$$

The following equations are considered to calculate the turbulence of kinetic energy (K) and frequency (ω):

$$\frac{\partial}{\partial x_i}=\left(Ku_i\right)=\frac{1}{\rho}\left(\frac{\partial}{\partial x_j}\left(\Gamma_k\frac{\partial k}{\partial x_j}\right)+\hat{G}_k-Y_K+S_K\right) \tag{25}$$

$$\frac{\partial}{\partial x_i}\left(\rho\omega u_i\right)=\frac{1}{\rho}\left(\frac{\partial}{\partial x_j}\left(\Gamma_\omega\frac{\partial\omega}{\rho x_j}\right)+\hat{G}_\omega-Y_\omega+D_\omega+S_\omega\right) \tag{26}$$

where G_k and G_ω are, respectively, the generation of (k) and (ω), Y_k and Y_ω are, respectively, the dissipation of kinetic energy and (ω) due to the turbulence. Γ_k is the effective diffusivity of K, and Γ_ω the effective diffusivity of (ω). The value of Γ_k is evaluated as follows:

$$\Gamma_K=u+\frac{u_t}{\sigma_k} \tag{27}$$

$$\Gamma_\omega=u+\frac{u_\omega}{\sigma_\omega} \tag{28}$$

where G_k and G_ω are, respectively, the generation of (k) and (ω), Y_k and Y_ω are, respectively.

2.2.3 Boundary condition

The boundary condition is calculated and assumed to be fully developed. The value of heat flux adopted is constant and at the importance of 1000 W/m^2. From the perspective of flow direction, the temperature gradient, as well as the velocity gradient, are zero. The working fluid is water, and its thermophysical properties are constant. At the inlet tube, thermal development and hydrodynamic fully developed are considered. The channel in the computational domain is considered 3-D, and the boundary condition is evaluated as depicted in Table 2.

Table 2
Boundary conditions

Boundary Conditions	Description
Inlet	$\frac{\partial u}{\partial z}=\frac{\partial v}{\partial z}+\frac{\partial w}{\partial z}=\frac{\partial T}{\partial z}=0$ u
Wall (no slip)	$u=v=w=0, T=T_w, q_w=1000\,w/m^2$
Vortex generator	$u=v=w=0, \frac{\partial T}{\partial y}=0$
outlet	$\frac{\partial u}{\partial z}=\frac{\partial v}{\partial z}=\frac{\partial w}{\partial z}=0, \frac{\partial T}{\partial z}=0\ \mathrm{Pressure}=p_{atm}; \frac{\mu}{\mu_t}=10$
Mean velocity and mean temperature	$u=u_{m_{in}}, v=w=0, Tm_{in}=298K$

2.3 Data Reduction Analysis

The following equation is provided to assess the flow and heat transfer parameters in the test channel:

Heat transfer coefficient:

$$h_{ave}=\frac{Q}{\Delta T\times A} \tag{29}$$

$$Q=\dot{m}Cp(T_{out}-T_{in}) \tag{30}$$

The velocity inlet is determined as follows:

$$u_{in}=\frac{\mathrm{Re}\,\mu}{\rho D_h} \tag{31}$$

The average Nusselt number:

$$Nu=\frac{hD_h}{K} \tag{32}$$

Where D_h refers to the hydraulic diameter of the tube which is evaluated as follows;

$$D_h = \frac{4A}{P} \tag{33}$$

where *A* and *P* are referred respectively to the cross-section area and the wetted perimeter. The friction factor can be calculated using the following formula:

$$f = \frac{2D_h \Delta P}{2\rho u^2} \tag{34}$$

The channel's hydraulic and thermal characteristics were compared using performance evaluation criteria (*PEC*), which can be calculated as demonstrated below:

$$PEC = \frac{\left(Nu/Nu_o\right)}{\left(f/f_o\right)^{(1/3)}} \tag{35}$$

3. Result and Discussion

3.1 Grid Independence Test

Grid independence test was carried out under several hexahedral elements to ensure the quality of the result under the balance of mesh size, computation cost and the requirement of Y^+. It was found that the cell size at 748,720, 909,160 and 1,195,950 indicated, respectively, 80.2440, 81.2440 and 81.2439 of *Nu*, which reveals that the difference between results is not significant as seen in Table 3.

Table 3
Grid independent test

Grid No.	Grid nodes	*Nu*	*e* %	*u* (m s^{-1})
1	748,720	126.1712	-	0.2675
2	909,160	127.1013	0.73717	0.2681
3	1.195,950	127.8551	0.59307	0.2688

Therefore, the mesh under 748,720 was adopted to save time and componential cost. The value of Y^+ at an inlet velocity value of 0.75 m/s and different angles and geometrical cross-sections are listed in Table 4. The percentage error is estimated using the following equation:

$$e\% = \frac{Q - Q_{n-1}}{Q_{n-1}} \tag{36}$$

Table 4
The value of Y^+ at different angles and geometrical cross-sections

Twisted angle (degree)	Y^+ value		
	Entry section	Lobe swirl	Test section
90	4.14	4.15	3.98
180	3.66	3.69	3.48
270	4.24	4.31	4.04
360	3.67	3.99	4.04

3.2 Validation of Numerical Study

To validate the current numerical study, a comparison between the Nusselt number and friction factor with Jafari *et al*., [30] experimental study and several theoretical correlations such as; Dittus-Boelter Eq. (37) and Seider-Tate Eq. (38) in terms of *Nu*. On the other hand, the correlations Blasius Eq. (39), Pertukhov Eq. (40) and Vatankhah Eq. (41) were adopted to study the comparison of the friction factor coefficient. Figure 7 clearly show that the current numerical study result is considered reliable at a relative deviation, respectively 2.47%, 2.6% and 7.6%, with Jafari *et al*., [30] experimental, Seider-Tate and Dittus-Boelter. Regarding the friction factor, the numerical result presented a good agreement at the deviation of 3.35%, 8.63%, 8.8% and 3.06%, respectively, compared with Jafari *et al*., [23] experimental, Blasius, Petukhov and Vatankhah in friction factor. The well-known Dittus-Boelter and Seider-Tate.

$$Nu = 0.023\,\mathrm{Re}_b^{4/5}\,p_r^{0.4} \tag{37}$$

The correlation is validated at the slight temperature difference (T_{wall}-T_{avg}) all the properties should be estimated at the average temperature (T_{avg}).

$$Nu = 0.027\,\mathrm{Re}_b^{4/5}\,p_b^{1/3}\left(\frac{\mu}{\mu_s}\right)^{0.14} \tag{38}$$

where μ and μ_s refer to the fluid viscosity at the bulk temperature and the wall surface. The correlation related to the friction factor adopted as the following:

$$f = 0.316\,\mathrm{Re}_b^{-1/4} \tag{39}$$

$$f = (0.79 * \ln(\mathrm{Re}_b) - 1.64)^{-2} \tag{40}$$

$$\frac{1}{\sqrt{f}} = 0.8686 * \ln\left(\frac{0.4587 * \mathrm{Re}}{(s-0.31)^{\frac{s}{s+0.9633}}}\right) where \ldots s = 0.124 * \mathrm{Re}\frac{\varepsilon}{D} + \ln(0.4587 * \mathrm{Re}) \tag{41}$$

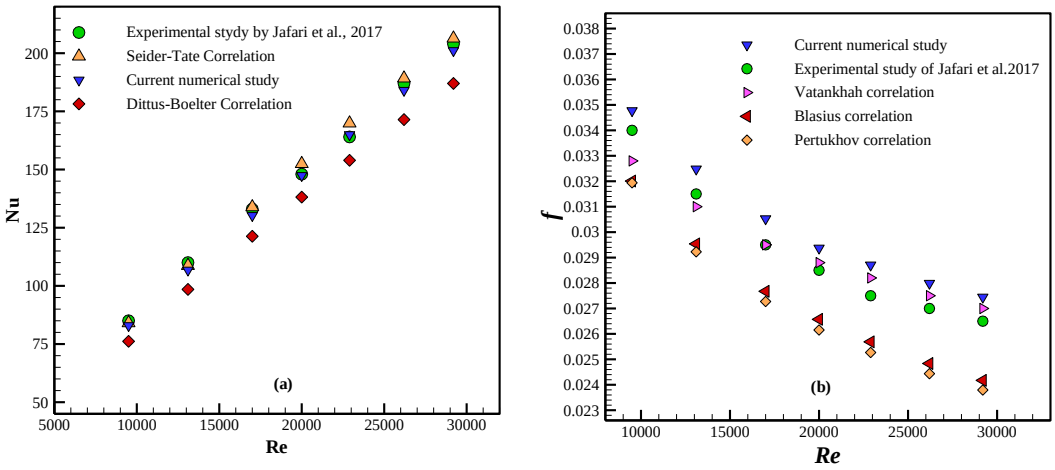

Fig. 7. Comparison between experimental correlations and current numerical results for a plane tube

3.3 The Effect of Beta Transition under Different Variables

As seen in Figure 8(a), the result revealed that the growth of the lobe area developed faster within the beginning of the transition part when (n < 1), and in case the transition multiplier became close to one, the lobed area developed faster at the end of the transition part. According to Figure 8(b), the twisting shape grows more quickly at the beginning and the end of the transition part at the values of (t < 1) and (t > 1), respectively. In terms of (t = 1), the twisting cross-section development is constant with respect to the length (geodesic).

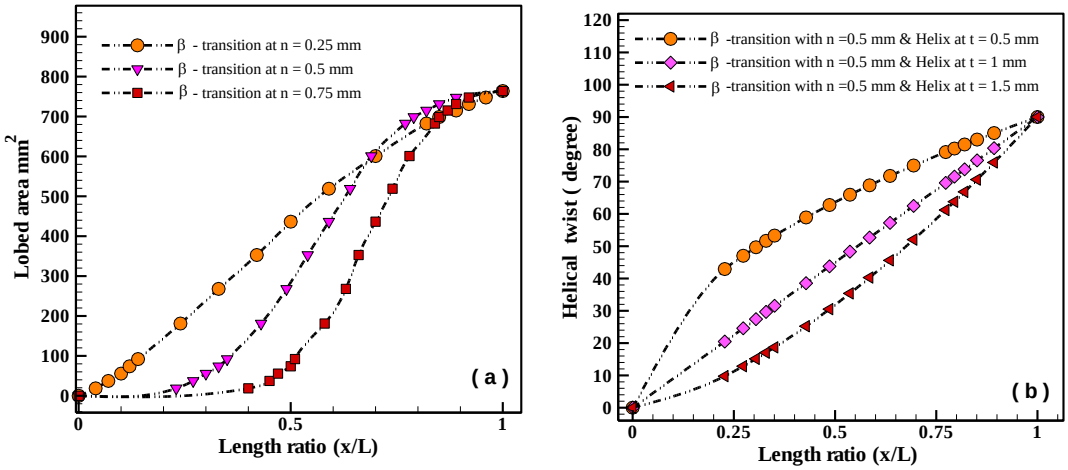

Fig. 8. The impact of (a) several transition multipliers on lobe area growth and (b) different values of a variable helix on twisting development

3.4 The Effect of Twisted Angles on Heat Transfer and Thermal Performance

The current study aimed to examine the heat transfer improvement and fluid flow behaviour using the four-lobed swirl generators under several angles. Figure 9(a) and 9(b) showed the effect of Four-lobe swirl generation at different angles with a variation of *Nu* and friction factor versus a different *Re*. The numerical study proved that the four-lobed swirl generator improves the heat transfer in all case studies with an augmentation in friction factor. The result also demonstrates the highest heat transfer associated with the angle (360°). As expected, it is attributed to the improvement in flow

fluctuation and mixing caused by the intensity of the swirl. It can be explained by the design feature of the four-lobe swirl generator with an angle of 360º caused a rapid change in swirl intensity, leading to a significant fluctuation of the flow between the wall and the core of the tube. It is expected that the increased inclination angle of 450º compared with others caused a decrease in swirl intensity, which is considered the main reason for reduced heat transfer. The Nusselt number (*Nu*) increases with Re in this regime, primarily due to the greater velocity gradients and enhanced convective effects. Furthermore, the stirring attribute of turbulent flow together with the characteristic curvature of lobe cross-section, have a considerable impact on heat transfer improvement, especially at a high *Re*. The highest heat transfer value at the twisted angle of 360 is 38%. Figure 9(b) depicts the variation of the friction factor at a different twisted angle and *Re*. The result revealed that the friction factor increases as the twisted angle increases. Moreover, the increase in *Re* led to a decrease in the friction factor. The result also illustrates the value of the fraction factor from 7% - 28% greater than the smooth tube. Although the increase in *Re* and twisted angle led to increasing heat transfer, the increase in friction factor can limit this improvement. The result depicted that the Re directly impact the heat transfer and pressure loss. Therefore, the result proved that the increase in Reynolds number leads to an increase in heat transfer and a reduction of the friction factor.

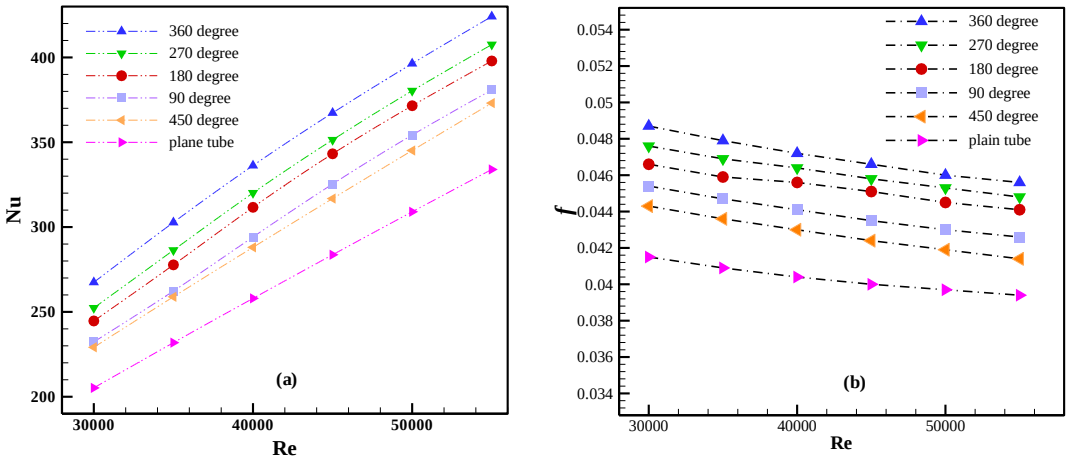

Fig. 9. The impact of several twisted angles on (a) heat transfer (b) friction factor at a different range of Reynolds numbers

A comparison between the heat transfer and friction factor at the smooth channel and after improvement is considered to study the lobe swirl generator's applicability at various parameters. Therefore, the value of heat transfer Nu/Nu_p and the value of friction factor f/f_p are considered. As shown in Figure 10(a) and 10(b), The result indicates the heat transfer enhancement by the factor from 1.1 to 1.33 with a slight increase in friction factor ratio value. Moreover, the result showed the highest heat transfer value with the twisted angle of (θ = 360º) and *Re* of 35,000. The result is highly consistent with Jafari *et al*., [43] observation. The result also indicated the worst value of Nu/Nu_p in the case of the angle at 450 º; it can be attributed to the highly sharp slope in this angle caused flow retardation, leads a reduction in swirl flow. It can be observed that rising the Reynolds number improves the values of f/f_p for all investigated swirl generators, indicating a nonlinear relationship between the Nusselt Number and the Reynolds Number.

To assess the system's performance in a thermal application, the ratio between the heat transfer value and the friction factor value is considered. Therefore, the performance evaluation criteria (*PEC*) technique an applied. If the value of *PEC* is greater than 1, the heat transfer improvement is higher than the friction factor and vice versa. A *PEC* greater than one revealed that the improvement in heat

transfer is more than the effect of the friction factor as examined in the literature [51]. The increase in *Re* with the rise in twisted angle can limit the thermal performance due to the augmentation of the friction factor.

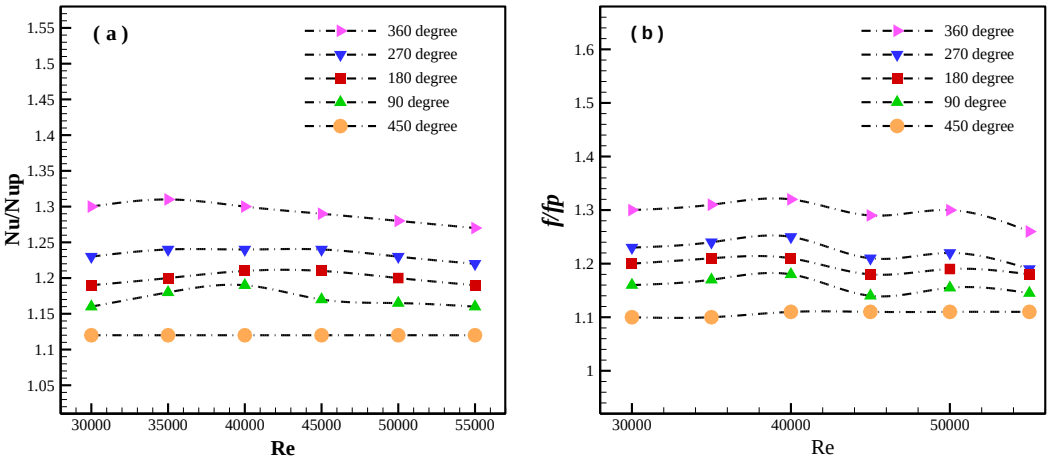

Fig. 10. Variation of Reynolds number versus (a) the ratio of Nusselt number Nu/Nu_p and (b) the ratio of friction factor f/f_p

As shown in Figure 11, the maximum value of thermal performance was 1.2 at the *Re* of 35,000 due to the impact of the friction factor. From the perspective of the effect of the Reynolds number on thermal performance. The thermal performance of swirl flow is higher at a lower Reynolds number. It can be attributed to the stronger viscosity at the reduction of Reynolds number. On the other hand, explaining the characteristics of a lobed swirl generator associated with turbulent flow is quite complex. Therefore, A polynomial relation between the thermal performance and the Reynolds number has been observed. The fluctuation of the flow due to the mechanism of the lobed swirl generator and the high turbulent intensity of the flow regime are considered the main factors that make the lobed swirl device more efficient at low Reynolds numbers due to diminishing returns in heat transfer relative to the increasing pressure loss. The improvement in thermal performance observed in the present research implies that the four-lobe swirl generator might significantly improve the efficiency of HVAC systems, particularly in energy-intensive contexts like commercial buildings.

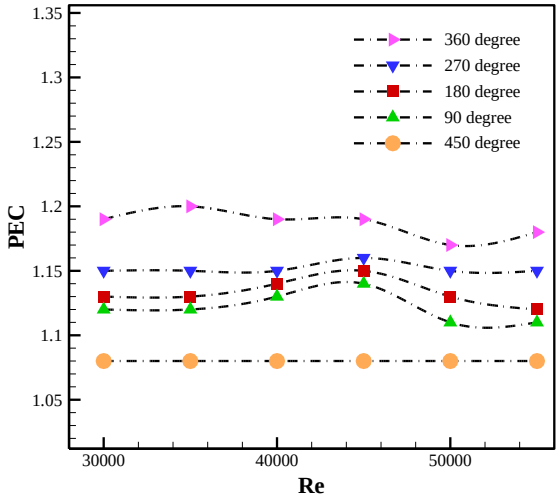

Fig. 11. PEC at different twisted angles and *Re*

3.5 The Effect of Different Multipliers (n) on Heat Transfer

As mentioned above, applying the transition multiplier led to controlling the intermediate area development. The multiplier values adopted in the current numerical study are (0.25, 0.5, and 0.75 mm). Figure 12(a) and 12(b) shows the variation of the *Nu* and friction factor of the lobed swirl generator at the effect of the transition multiplier. It can be noted that the transition part with a beta transition value of *n* = 0.25 mm shows the highest *Nu* and friction factor. It can be attributed to the lobe area's faster growth near the beginning of the transition part, which led to an increase in the turbulent flow and improved heat transfer. Because all the values are close and less than one, there is no considerable change in heat transfer. It is worth implying that the heat transfer with a reduction of transition multiplier (*n*) presented the heat transfer up to 40% with an acceptable increase in friction factor at 16%.

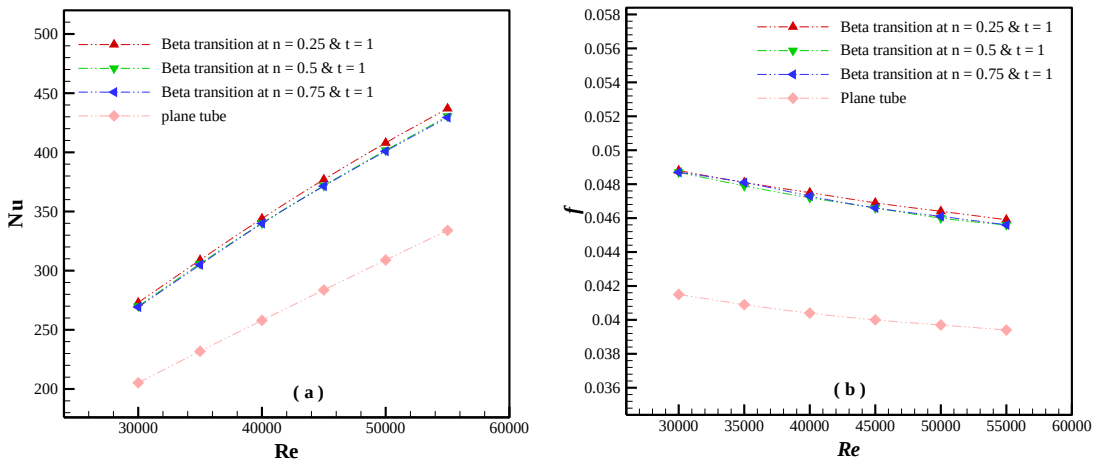

Fig. 12. Effect of different beta transition multipliers on (a) heat transfer (b) friction factor at constant variable helix and twisted angle of 360°

To study the impact of different transition multiplier values on thermal performance and flow fields, a comparative study for the four-lobe swirl generator under several values of transition multiplier and *Re* is carried out. Therefore, the transition multiplier of *n* = 0.25, 0.5, and 0.75 mm was also adopted to study their effect on thermal performance criteria. Figure 13 proved that all transition multipliers considerably impact thermal performance improvement. The result also revealed that the system's thermal performance slightly increased with a reduction of the transition multiplier value. It can be explained by the growth of the lobe area at the transition part region as the transition multiplier value set less than 1. The performance evaluation criteria at *PEC* of 1.25 is located at the transition multiplier value of 0.25 mm. It can be explained by the fact of the increase in tangential velocity as a result of multiplier (*n*) decreasing, and this phenomenon was proved by Ariyaratne *et al.,* [37]. A high *PEC* value implies a high rate of heat transfer as examined Nfawa *et al.,* [52].

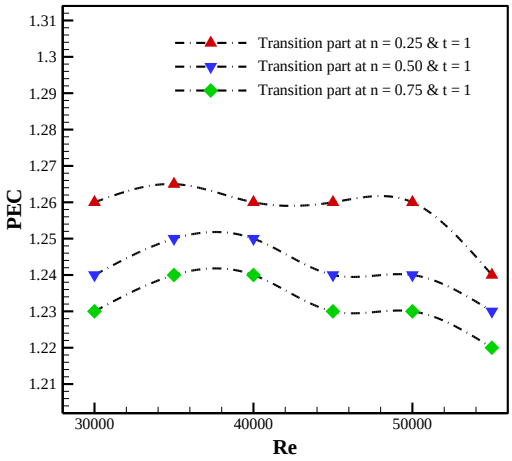

Fig. 13. Thermal performance value at different transition multipliers and variable helix

3.6 The Effect of a Variable Helix (t) on Heat Transfer and Thermal Performance

The power law or variable helix (*t*) is an innovation to control the curvature of the transition part during its development as performed by Li [47]. The variable helix (*t*) with different values of *t* = 0.5, 1, and 1.5 on heat transfer and friction factor were considered. These parameters were performed at a twisted angle of 360º and a transition multiplier of 0.25 mm. As shown in Figure 14(a) and 14(b), the variable helix at the value of 1 (geodesic) presented the highest heat transfer improvement with a slight friction factor increase. As expected, the transition part at constant twisted growth with respect to distance (geodesic) results in efficient swirling flow, and this corresponds with the finding of the study by Li *et al.,* [42].

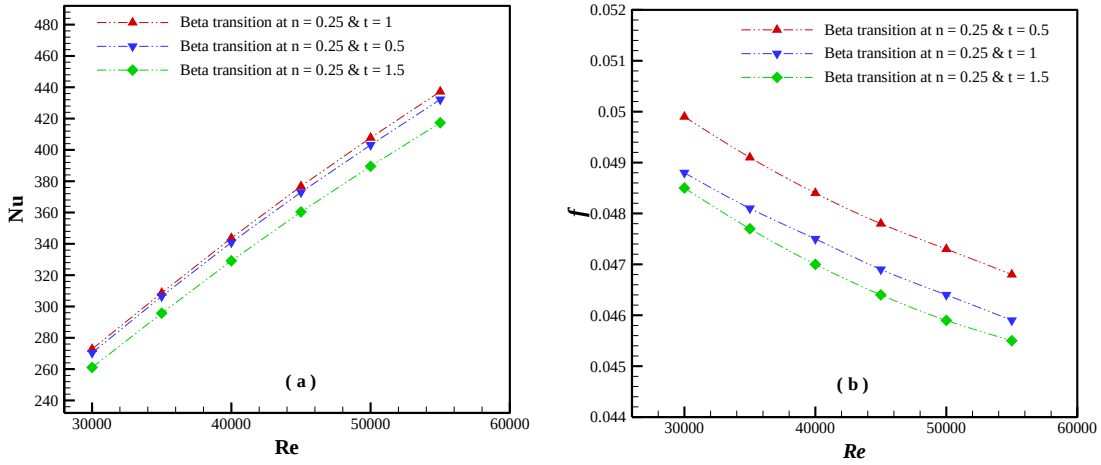

Fig. 14. Effect of Beta transition at multiplier (*n* = 0.25), lobed swirl angle (θ = 360º) and different Helix variable (*t* = 0.5, 1, 1.5) on (a) heat transfer (b) friction factor

It is worth mentioning that the lobed swirl generator has been designed with two essential transition parts. These components have been developed gradually changed from a lobed circular shape (no lobe) to a lobed cross-section at the entry section of the transition part and from a lobed cross-section to a circular shape at the exit transition part to a voided the sudden change in the cross-section between developed entry section and lobed swirl generator itself to prevent the augmentation of pressure losses as a result of cross-sections sudden changed. In comparison with

the previous studies, the lobed swirl generator is equipped with two essential transition parts thus, the pressure loss penalty is dropped noticeably. The lobed device itself was investigated under different twisted angles as the first targeted outcome of the current numerical study. The result revealed that increased twisted angle led to increased heat transfer. It is worth mentioning that the improvement in thermal performance requires reducing pressure loss and improving heat transfer capacity. Therefore, the friction factor value (f/f_p) takes place. The result presented an augmentation in friction factor as the twisted angle of the lobed swirl generator increased. Consequently, the performance evaluation criteria (PEC) are considered to obtain the balance between enhanced heat transfer and the associated pressure loss. The study concluded that a twisted angle of 360^o led to better thermal performance. It may be clarified by the fact that there is less friction and pressure loss when heat transmission is increased at this angle. Also, the PEC considered in the investigation of transition Multipliers (n) and under different values to adopt the balance between the improvement in heat transfer and the impact of pressure loss. The result concluded that the decrease in n-value led to an increase in thermal performance. It can be explained by the fact that the transition area grows fast as the transition multiplier value decreases, which leads to promoting heat transfer and reduces pressure loss. Moreover, it can explain the improvement in heat transfer by the augmentation of tangential velocity as the transition Multiplier value decreases. The result is highly consistent with the findings of Najafian *et al.,* [34].

According to lobed number impact, the current study performed the swirl under the 4-lobe. Krishna *et al.,* [53] revealed that the lobed swirl generator of (10-lobe) led to a reduction in the pressure loss compared with all lobed numbers investigated. Firoozeh *et al.,* [54] reported that the groove angle is a vital step in terms of improving heat transfer. Yan *et al.,* [26] revealed that the optimum swirl effectiveness was indicated at 4-lobed. Compared with the results, it attributed the difference in the effect of the transition part developed section and pitch-to-diameter of (P:D = 8), which was stated as the optimum design. From the geometrical cross-sectional view, the lobe swirl generator has different lobe numbers and shapes, namely, 3-lobe, 4-lobe, 5-lobe, four triangular lobes, twisted oval and twisted tri-lobe, tri-lobe tube with crooked tape, a helical coil with lobe cross-section, lobe swirl generator with Y-tape twisted tubes insert. Jafari *et al.,* [30] also examine the impact of a 4-lobe swirl on thermal performance. The study presents considerable heat transfer associated with (l =4) and (ϑ = 360º). On the other hand, 5-lobe at (l =4) and (ϑ = 360º) showed an enhancement in heat transfer by the value of 85%, with increases in friction factor (f) by up to 52% as discovered by Jafari *et al.,* [31]. The comparison between 4-lobe swirl devices at lengths of 0.6 m and 0.4 m on fluid flow was studied by Li *et al.,* [42]. The study was performed at the angles of 360º and 450º. The study proved that the pipe length of 0.4 m with (ϑ = 360º) significantly affected the swirl induction, with an applicable level of pressure loss. By comparing the current result with previous studies, it can be concluded that the parameters adopted in different studies have several impacts on heat transfer, thermal performance and fluid flow. Large surface area, and shapes such as Fins, ribs, or swirl generators introduce turbulence, improving convective heat transfer. Compared to a smooth pipe, a corrugated pipe improves heat transmission by increasing surface area and turbulence. The small diameter of the tube has a considerable impact on heat transfer compared to a large tube due to thinner thermal boundary layers and faster velocities associated with a small diameter. From the prospect of environmental impact, the adoption of four-lobe swirl generators in thermal systems can have a profound environmental impact. By enhancing energy efficiency and reducing emissions, they align with global efforts to combat climate change and transition to sustainable energy solutions. Their integration into diverse industries can significantly reduce greenhouse gas emissions, making them an important technology for a greener future.

3.7 Sensitivity Analysis: One-at-a-Time (OAT) Approach

The One-at-a-Time (OAT) sensitivity analysis is a method to evaluate the effect of changing one input variable while keeping all other variables constant. It is a simple and effective technique for understanding how a single variable influences the output (in this case, the Nusselt number) when other factors are fixed. Analysing the sensitivity of the Nusselt number (*Nu*) to velocity (*v*) in a typical pipe flow. We will perform a sensitivity analysis using Ansys Workbench 2020R2. The sensitivity analysed varies velocity (*v*) over a range (0.6828 to 1.2518 m/s) while keeping diameter (D), density (ρ), and viscosity (μ) constant. It is worth mentioning, that the study aimed to perform the lobed swirl generator under different twisted angles from (90 to 450). The results revealed that the lobed swirl at a twisted angle of 360 degrees exhibited superior thermal performance compared to all other cases investigated. Therefore, the sensitivity analysis focuses on this angle as the optimal case. Calculating the percentage sensitivity for each change in the Nusselt number is presented in Table 5.

Table 5
The sensitivity analysis of Nusselt number at twisted angle 360^{o} over different velocity

Reynolds number (*Re*)	Velocity (*v*)	Nusselt number (*Nu*)	Change in *Nu*	Percentage Sensitivity (%)
30,000	0.6828	267.4579	-	-
35,000	0.7966	302.7486	35.5	13.1%
40,000	0.9104	336.2742	33.5	11.1%
45,000	1.0242	367.319	31.1	9.2%
50,000	1.138	396.3796	29.7	7.9%
55,000	1.2518	424.1243	27.7	6.9%

The result showed that the Nusselt number increased with the increase of Reynolds number. The sensitivity declines as the velocity increases, meaning that the Nusselt number becomes less sensitive to changes in velocity at higher values. At low velocity (0.7966 m/s); The Nusselt number is highly sensitive to changes in velocity (about 13.1% increase), which is common at lower Reynolds numbers where convection is still developing, and small changes in velocity cause significant changes in the convective heat transfer. On the other hand, at high Velocities (0.9104 to 1.2518 m/s), the Nusselt number is less sensitive to changes in velocity, with percentage sensitivity dropping as velocity increases. This is because at higher Reynolds numbers, the convective heat transfer becomes more efficient, and further increases in velocity lead to smaller incremental changes in heat transfer. In a one-at-a-time (OAT) sensitivity analysis, varying the flow velocity reveals a distinct relationship between velocity and the Nusselt number. Specifically, the Nusselt number increases with rising velocity; however, its velocity sensitivity diminishes as the flow transitions to a more turbulent regime, characterized by higher Reynolds numbers. This analysis proves valuable in quantifying the influence of a single parameter, in this case, velocity, on the output variable, the Nusselt number.

3.8 Tangential and Axial Velocities Pattern

The lobed swirl device has a curvature cross-section leading to centrifugal generated toward the test tube downstream, causing a vigorous tangential velocity formed near the wall as well as axial velocity concentrated at the core. As shown in Figure 15, the contour proved the ability of four- the lobe to produce tangential velocity noticeable around the wall under different twisted angles. The tangential velocity is zero at the tube centre, increasing as it gets closer to the wall and decreasing again to zero when it directly contacts the wall. The contours showed a clear quadrangular shape near the entrance of the lobe swirl and gradually faded towards the test tube exit, which is considered

a characteristic of a four-lobe swirl device. From the axial velocity perspective, the highest axial velocity is concentrated in the core and decreases as the tube distance increases for all twisted angles investigated. In comparison between the twisted angles, it is worth mentioning that the twisted shape at *x/L* = 0 is more pronounced with the angle of 360º instead of 90º for both velocities. Therefore, produces more flow fluctuation and heat transfer enhancement. In other words, the swirl formed stronger at the beginning of the pipe and gradually faded at the end of the tube downstream. The contour proved the ability of the four-lobe swirl generator to produce azimuthal velocity noticeable around the wall under different twisted angles. The tangential velocity is zero at the tube centre, increasing as it gets closer to the wall and decreasing again to zero when it directly contacts the wall. The contours showed a precise quadrangular shape near the entrance of the lobe swirl.

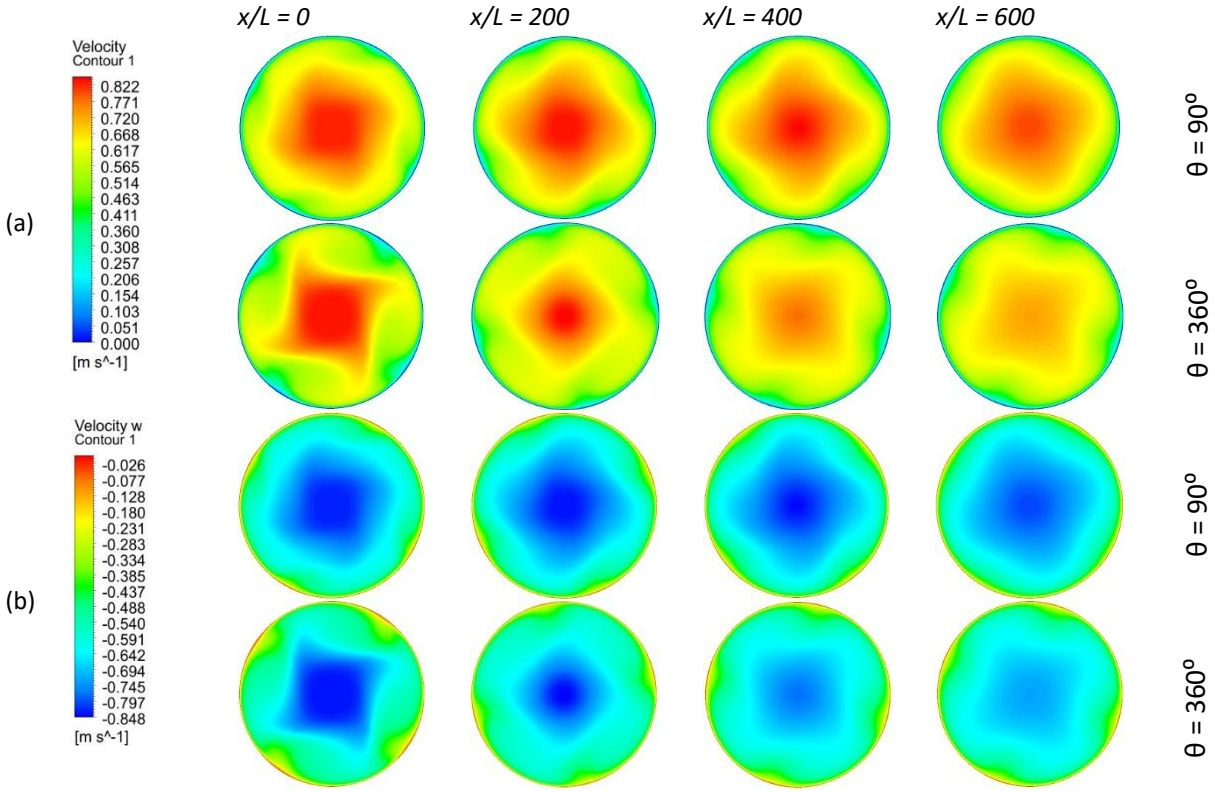

Fig. 15. Tangential velocity and axial velocity distribution at different twisted angles, and distance under *Re* of 35,000

3.9 Streamline

Figures 16(a), 16(b) and 16(c) depict 3-D streamlined contours to illustrate the spiral swirl flow pattern from an isometric perspective, whereas Figures 16(d), 16(e) and 16(f) show swirl flow behaviour in the front view. The outcome was performed at different angles of 90°, 270° and 360°. The result was carried out at a *Re* of 55,000 and geometry contour points of 100 streamlines. The result demonstrates that the lobed swirl generator under different angles can create two essential types of swirling flow. Axial velocity is concentrated in the core and increased in the lobed cross-section region (red zone). The second swirl flow is tangential velocity generated adjacent to the wall.

The result also proved that the contact between the axial and tangential velocity is the main reason for creating small-scale vortices between the core and the wall. The contour revealed that the increase in twisted angle led to an increase in the scale vortices. The streamlined distribution confirms that the rise in twisted angle led to more fluctuation in flow and mixing. Consequently, promotes the

performance of heat transfer. Although the current result performed at the same *Re*, the lobe swirl at the angle of 360º presented the superior velocity by the value of 6.87% compared with the angle of 90º. The longitudinal vortices induced by the lobed swirl generator at a twisted angle of 360 degrees are more intensive, which improves synergy between the velocities and the temperature gradient, causing better thermal performance. The result also presented swirl flow in smooth channels due to the characteristics of different twisted angles of the lobed swirl generator. It can be observed that the fluid adjacent to the wall swirls continuously and dramatically disturbs the boundary layer. It has improved the heat transfer rate due to mixing between the fluid flow near the wall (hot water) and at the core (cold water).

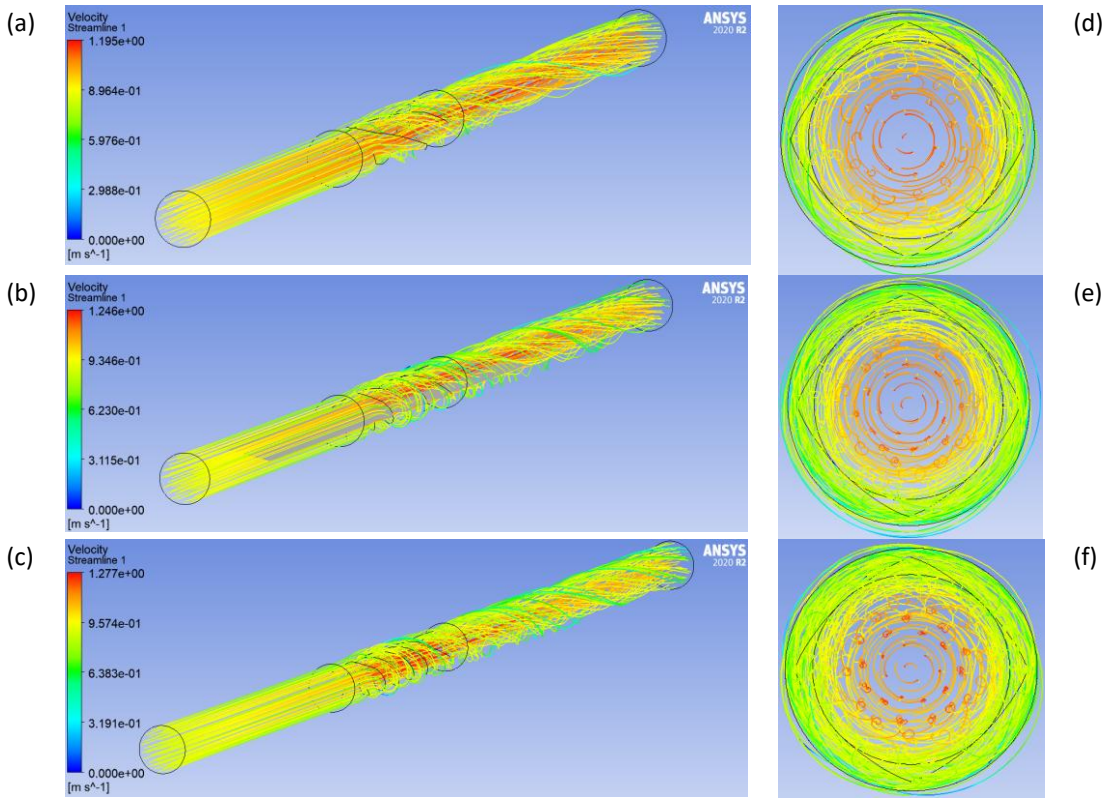

Fig. 16. 3-D streamline contours of the four-lobed swirl generator under different angles (a) 90º, (b) 270º, and (c) 360º

4. Motivation of the Study

Due to the poor heat transfer associated with smooth channels, several techniques have been developed to generate swirl flow within circular tubes. It can divide the swirl flow induced within a circular tube into different crucial categories: the swirl flow generated by the propeller-type swirl as investigated in the study by Ali *et al.,* [55], swirl flow by converting the circular tube to several types of curved tubes such as:

i. helical coil
ii. bend tube
iii. serpentine rube
iv. spiral
v. twisted tubes as mentioned by Ghobadi *et al.,* [56] and creating swirl flow by inserting device techniques as performed by Azhari *et al.,* [57].

According to the present study, the lobed swirl generator has effective properties, represented by its ability to improve the overall swirl intensity and reduce pressure loss due to the advantage of its transition parts as presented by Ariyaratne *et al.,* [37]. Therefore, applying this feature on smooth channels can considerably enhance heat transfer in many thermal applications, which is the motivation behind the current study. In addition, exploring the thermal characteristics of this device for more understanding is also the targeted outcome. In the present work, the thermal performance of a four-lobed swirl generator was investigated numerically under different parameters such as twisted angles (ranging from 90º to 450º), transition multiplier values (ranging from *n* = 0.25 to 0.75 mm), and variable helix dimensions (*t* = 0.5 to 1.5 mm), which considered a unique study in the thermal application field. Consequently, it is extremely important to point out the gaps in the aforementioned research and highlight the specifications that the lobed swirl generator and its transition components must fulfil for the thermal application.

5. Conclusion

In the present numerical study, the effect of a four-lobed swirl device with its transition parts on thermal performance and fluid field has been carried out. The geometry studied can be divided into two main practical parts. The lobed swirl device was performed under a fixed length at 0.2 m, beta transition at the multiplier of (*n* = 0.5 mm) and different twisted angles from (90^{o} to 450^{o}). The second vital section is the Transition part of the entry and exit transition sections of 0.1 m. This part was investigated at different transition multipliers (*n* = 0.25, 0.5 and 0.75 mm) and several variable helixes (*t* = 0.5, 1, 1.5 mm). The turbulent water flow induced by the lobed swirl was generated in the *Re* ranges of 30,000 to 55,000. After implementing the simulation, the following results have been obtained:

i. The result showed that raising the twisted angle significantly boosted the heat transmission. Additionally, the lobed swirl generator with the angle of (θ = 360º) had the best thermal performance with PEC = 1.21 and the largest heat transfer value up to 28.78.
ii. The outcome shows a slight enhancement in thermal performance by a factor of 1.26, with the multiplier transition component being reduced to values of (n = 0.25 mm) and (t = 1).
iii. There is no impact on thermal performance by decreasing or increasing the variable helix value, therefore the result confirmed that the (t =1) is the optimum.
iv. The result revealed the capability of a lobed swirl generator under different parameters to produce a centrifugal force, which is the main reason for heat transfer enhancement.
v. The findings provide a unique technique for increasing energy efficiency by demonstrating that the four-lobe swirl generator is suitable for various industrial applications, including heat exchangers and vehicle cooling.

Acknowledgements
The research was funded under the MySIP grant scheme no. 5540547 from Ministry of Higher Education Malaysia.

References
[1] Jiang, Chen, Bofeng Bai, Haibo Wang, Jiqing Shi, Xiaoying Tang, and Wenxue Zhou. "Heat transfer enhancement of plate heat exchangers with symmetrically distributed capsules to generate counter-rotating vortices." *International Journal of Heat and Mass Transfer* 151 (2020): 119455. https://doi.org/10.1016/j.ijheatmasstransfer.2020.119455

[2] Hilo, Ali Kareem, Antonio Acosta Iborra, Mohammed Thariq Hameed Sultan, and Mohd Faisal Abdul Hamid. "Effect of corrugated wall combined with backward-facing step channel on fluid flow and heat transfer." *Energy* 190 (2020): 116294. https://doi.org/10.1016/j.energy.2019.116294

[3] Mousa, Mohamed H., Nenad Miljkovic, and Kashif Nawaz. "Review of heat transfer enhancement techniques for single phase flows." *Renewable and Sustainable Energy Reviews* 137 (2021): 110566. https://doi.org/10.1016/j.rser.2020.110566

[4] Mousavi Ajarostaghi, Seyed Soheil, Mohammad Zaboli, Hossein Javadi, Borja Badenes, and Javier F. Urchueguia. "A review of recent passive heat transfer enhancement methods." *Energies* 15, no. 3 (2022): 986. https://doi.org/10.3390/en15030986

[5] Tang, Xinyi, Xianfeng Dai, and Dongsheng Zhu. "Experimental and numerical investigation of convective heat transfer and fluid flow in twisted spiral tube." *International Journal of Heat and Mass Transfer* 90 (2015): 523-541. https://doi.org/10.1016/j.ijheatmasstransfer.2015.06.068

[6] Li, Guozhen, Philip Hall, Nick Miles, and Tao Wu. "Improving the efficiency of 'Clean-In-Place'procedures using a four-lobed swirl pipe: A numerical investigation." *Computers & Fluids* 108 (2015): 116-128. https://doi.org/10.1016/j.compfluid.2014.11.032

[7] Rashidi, Saman, Mohammad Hossein Kashefi, and Faramarz Hormozi. "Potential applications of inserts in solar thermal energy systems–a review to identify the gaps and frontier challenges." *Solar Energy* 171 (2018): 929-952. https://doi.org/10.1016/j.solener.2018.07.017

[8] Ariyaratne, C., and T. F. Jones. "Design and optimization of swirl pipe geometry for particle-laden liquids." *AIChE journal* 53, no. 4 (2007): 757-768. https://doi.org/10.1002/aic.11122

[9] Brar, Lakhbir Singh, and J. J. Derksen. "Revealing the details of vortex core precession in cyclones by means of large-eddy simulation." *Chemical Engineering Research and Design* 159 (2020): 339-352. https://doi.org/10.1016/j.cherd.2020.04.030

[10] Stroh, A., K. Schäfer, P. Forooghi, and B. Frohnapfel. "Secondary flow and heat transfer in turbulent flow over streamwise ridges." *International Journal of Heat and Fluid Flow* 81 (2020): 108518. https://doi.org/10.1016/j.ijheatfluidflow.2019.108518

[11] Gobinathan, Sashwin Nair, Azizuddin Abd Aziz, Ahmed Nurye Oumer, Mohd Yusof Taib, and Ahmad Basirul Subha Alias. "A Review on Heat Transfer Enhancement in a Heat Exchanger." *Journal of Advanced Research in Fluid Mechanics and Thermal Sciences* 122, no. 2 (2024): 130-145. https://doi.org/10.37934/arfmts.122.2.130145

[12] Shelare, Sagar D., Kapil R. Aglawe, and Pramod N. Belkhode. "A review on twisted tape inserts for enhancing the heat transfer." *Materials Today: Proceedings* 54 (2022): 560-565. https://doi.org/10.1016/j.matpr.2021.09.012

[13] Keklikcioglu, Orhan, and Veysel Ozceyhan. "Heat transfer augmentation in a tube with conical wire coils using a mixture of ethylene glycol/water as a fluid." *International Journal of Thermal Sciences* 171 (2022): 107204. https://doi.org/10.1016/j.ijthermalsci.2021.107204

[14] Chan, Kian Wui, Ishkrizat Taib, and Xin Yi Wong. "Flow Characteristics Effect on Different Blades Number of Radial Fan." *Semarak Journal of Thermal-Fluid Engineering* 2, no. 1 (2024): 1-8.

[15] Du, Shen, Ming-Jia Li, Ya-Ling He, and Sheng Shen. "Conceptual design of porous volumetric solar receiver using molten salt as heat transfer fluid." *Applied Energy* 301 (2021): 117400. https://doi.org/10.1016/j.apenergy.2021.117400

[16] Bulut, Murat, Maharshi Shukla, Satish G. Kandlikar, and Nedim Sozbir. "Experimental study of heat transfer in a microchannel with pin fins and sintered coatings." *Experimental Heat Transfer* 36, no. 7 (2023): 1099-1114. https://doi.org/10.1080/08916152.2023.2176566

[17] He, Ziqiang, Yunfei Yan, Ting Zhao, Shuai Feng, Xiuquan Li, Li Zhang, and Zhien Zhang. "Heat transfer enhancement and exergy efficiency improvement of a micro combustor with internal spiral fins for thermophotovoltaic systems." *Applied Thermal Engineering* 189 (2021): 116723. https://doi.org/10.1016/j.applthermaleng.2021.116723

[18] Salman, S., AR Abu Talib, S. Saadon, and MT Hameed Sultan. "Hybrid nanofluid flow and heat transfer over backward and forward steps: A review." *Powder Technology* 363 (2020): 448-472. https://doi.org/10.1016/j.powtec.2019.12.038

[19] Monfared, Roohollah Hosseini, Mohammadreza Niknejadi, Davood Toghraie, and Pouya Barnoon. "Numerical investigation of swirling flow and heat transfer of a nanofluid in a tube with helical ribs using a two-phase model." *Journal of Thermal Analysis and Calorimetry* 147, no. 4 (2022): 3403-3416. https://doi.org/10.1007/s10973-021-10661-1

[20] Bezaatpour, Mojtaba, and Mohammad Goharkhah. "Convective heat transfer enhancement in a double pipe mini heat exchanger by magnetic field induced swirling flow." *Applied Thermal Engineering* 167 (2020): 114801. https://doi.org/10.1016/j.applthermaleng.2019.114801

[21] Shlash, Bassam Amer Abdulameer, and Ibrahim Koç. "Turbulent fluid flow and heat transfer enhancement using novel Vortex Generator." *Journal of Advanced Research in Fluid Mechanics and Thermal Sciences* 96, no. 1 (2022): 36-52. https://doi.org/10.37934/arfmts.96.1.3652

[22] Wang, Dongyun, Artem Khalatov, E. Shi-Ju, and Igor Borisov. "Swirling flow heat transfer and hydrodynamics in the model of blade cyclone cooling with inlet co-swirling flow." *International Journal of Heat and Mass Transfer* 175 (2021): 121404. https://doi.org/10.1016/j.ijheatmasstransfer.2021.121404

[23] Gorelikov, E. U., I. V. Naumov, M. A. Tsoy, and V. N. Shtern. "Heat transfer in a centrifugal vortex tube." In *Journal of Physics: Conference Series*, vol. 2119, no. 1, p. 012065. IOP Publishing, 2021. https://doi.org/10.1088/1742-6596/2119/1/012065

[24] Shahsavar, Amin, Sajad Entezari, Ighball Baniasad Askari, Mehdi Jamei, Masoud Karbasi, and Mohammad Shahmohammadi. "Investigation on two-phase fluid mixture flow, heat transfer and entropy generation of a non-Newtonian water-CMC/CuO nanofluid inside a twisted tube with variable twist pitch: Numerical and evolutionary machine learning simulation." *Engineering analysis with boundary elements* 140 (2022): 322-337. https://doi.org/10.1016/j.enganabound.2022.04.022

[25] Omidi, Mohamad, Mousa Farhadi, and A. Ali Rabienataj Darzi. "Numerical study of heat transfer on using lobed cross sections in helical coil heat exchangers: effect of physical and geometrical parameters." *Energy conversion and management* 176 (2018): 236-245. https://doi.org/10.1016/j.enconman.2018.09.034

[26] Yan, Tie, Jingyu Qu, Xiaofeng Sun, Ye Chen, Qiaobo Hu, and Wei Li. "Numerical evaluation on the decaying swirling flow in a multi-lobed swirl generator." *Engineering Applications of Computational Fluid Mechanics* 14, no. 1 (2020): 1198-1214. https://doi.org/10.1080/19942060.2020.1816494

[27] Waware, Shital Yashwant, Sandeep Sadashiv Kore, Anant Sidhappa Kurhade, and Suhas Prakashrao Patil. "Innovative Heat Transfer Enhancement in Tubular Heat Exchanger: An Experimental Investigation with Minijet Impingement." *Journal of Advanced Research in Fluid Mechanics and Thermal Sciences* 116, no. 2 (2024): 51-58. https://doi.org/10.37934/arfmts.116.2.5158

[28] Kore, Sandeep Sadashiv, Manoj Kumar Chaudhary, Adhikrao Sarjerao Patil, and Vijay Dilip Kolate. "Computational study and enhancement of heat transfer rate by using inserts introduced in a heat exchanger." *Journal of Advanced Research in Fluid Mechanics and Thermal Sciences* 103, no. 1 (2023): 16-29. https://doi.org/10.37934/arfmts.103.1.1629

[29] Jafari, Kimia, Mohammad Hossein Fatemi, and Patrice Estellé. "Deep eutectic solvents (DESs): A short overview of the thermophysical properties and current use as base fluid for heat transfer nanofluids." *Journal of Molecular Liquids* 321 (2021): 114752. https://doi.org/10.1016/j.molliq.2020.114752

[30] Jafari, Mohammad, Mousa Farhadi, and Kourosh Sedighi. "Thermal performance enhancement in a heat exchanging tube via a four-lobe swirl generator: An experimental and numerical approach." *Applied Thermal Engineering* 124 (2017): 883-896. https://doi.org/10.1016/j.applthermaleng.2017.06.095

[31] Jafari, Mohammad, Mousa Farhadi, and Kourosh Sedighi. "An experimental study on the effects of a new swirl generator on thermal performance of a circular tube." *International Communications in Heat and Mass Transfer* 87 (2017): 277-287. https://doi.org/10.1016/j.icheatmasstransfer.2017.07.016

[32] Diabis, Farag A., Yazan Al-Tarazi, Norkhairunnisa Mazlan, and Eris Elianddy Supeni. "Thermal Performance of Four-Lobe Swirl Generator and its Transition Parts Under a Different Type of Nanofluids." *CFD Letters* 14, no. 11 (2022): 63-74. https://doi.org/10.37934/cfdl.14.11.6374

[33] Zaboli, Mohammad, Mehdi Nourbakhsh, and Seyed Soheil Mousavi Ajarostaghi. "Numerical evaluation of the heat transfer and fluid flow in a corrugated coil tube with lobe-shaped cross-section and two types of spiral twisted tape as swirl generator." *Journal of Thermal Analysis and Calorimetry* 147 (2022): 999-1015. https://doi.org/10.1007/s10973-020-10219-7

[34] Najafian, Mahyar, Ali Esmaeili, Amirfarhang Nikkhoo, Hui Jin, and M. R. Soufivand. "Numerical study of heat transfer and fluid flow of supercritical water in twisted spiral tubes." *Energy Sources, Part A: Recovery, Utilization, and Environmental Effects* 44, no. 3 (2022): 6433-6455. https://doi.org/10.1080/15567036.2022.2098421

[35] Jafari, Mohammad, Amir Farajollahi, and Heshmatollah Gazori. "The experimental investigation concerning the heat transfer enhancement via a four-point star swirl generator in the presence of water–ethylene glycol mixtures." *Journal of Thermal Analysis and Calorimetry* 144 (2021): 167-178. https://doi.org/10.1007/s10973-020-09408-1

[36] Esfe, Mohammad Hemmat, Hossein Mazaheri, Sayed Sajad Mirzaei, Ehsan Kashi, Mehrdad Kazemi, and Masoud Afrand. "Effects of twisted tapes on thermal performance of tri-lobed tube: An applicable numerical study." *Applied thermal engineering* 144 (2018): 512-521. https://doi.org/10.1016/j.applthermaleng.2018.07.106

[37] Ariyaratne, C., and T. F. Jones. "Design and optimization of swirl pipe geometry for particle-laden liquids." *AIChE journal* 53, no. 4 (2007): 757-768. https://doi.org/10.1002/aic.11122

[38] Bezaatpour, Mojtaba, and Hadi Rostamzadeh. "Energetic and exergetic performance enhancement of heat exchangers via simultaneous use of nanofluid and magnetic swirling flow: A two-phase approach." *Thermal Science and Engineering Progress* 20 (2020): 100706. https://doi.org/10.1016/j.tsep.2020.100706

[39] Rezaei, Arash, Sajed Hadibafekr, Morteza Khalilian, Ata Chitsaz, Iraj Mirzaee, and Hassan Shirvani. "A Comprehensive numerical study on using lobed cross-sections in spiral heat exchanger: Fluid flow and heat transfer analysis." *International Journal of Thermal Sciences* 193 (2023): 108464. https://doi.org/10.1016/j.ijthermalsci.2023.108464

[40] Hamdan, Mohammad O. "Decaying Swirl Flow Impact on Developing Laminar Pipe Flow."

[41] Patil, Rahul Harishchandra. "Fluid flow and heat transfer analogy for laminar and turbulent flow inside spiral tubes." *International Journal of Thermal Sciences* 139 (2019): 362-375. https://doi.org/10.1016/j.ijthermalsci.2019.01.036

[42] Li, Guozhen, Philip Hall, Nick Miles, and Tao Wu. "Optimization of a four-lobed swirl pipe for clean-in-place procedures." In *ICCE 2015: International Conference on Clean Energy*, p. 561. 2015.

[43] Jafari, Mohammad, Sadegh Dabiri, Mousa Farhadi, and Kurosh Sedighi. "Effects of a three-lobe swirl generator on the thermal and flow fields in a heat exchanging tube: an experimental and numerical approach." *Energy Conversion and Management* 148 (2017): 1358-1371. https://doi.org/10.1016/j.enconman.2017.06.074

[44] Ganeshalingam, Jeyakumar. "Swirl-induction for improved solid-liquid flow in pipes." PhD diss., University of Nottingham, 2002.

[45] Qazi, Salahuddin. *Standalone photovoltaic (PV) systems for disaster relief and remote areas*. Elsevier, 2016. https://doi.org/10.1016/B978-0-12-803022-6.00004-6

[46] Ariyaratne, Chanchala. "Design and optimisation of swirl pipes and transition geometries for slurry transport." PhD diss., University of Nottingham, 2005.

[47] Li, Guozhen. "Investigation of swirl pipe for improving cleaning efficiency in closed processing system." PhD diss., University of Nottingham, 2016.

[48] Raylor, Benjamin. "Pipe design for improved particle distribution and improved wear." (2000): 0497-0497.

[49] Li, Guozhen, Philip Hall, Nick Miles, and Tao Wu. "Improving the efficiency of 'Clean-In-Place'procedures using a four-lobed swirl pipe: A numerical investigation." *Computers & Fluids* 108 (2015): 116-128. https://doi.org/10.1016/j.compfluid.2014.11.032

[50] Oneissi, Mohammad, Charbel Habchi, Serge Russeil, Daniel Bougeard, and Thierry Lemenand. "Novel design of delta winglet pair vortex generator for heat transfer enhancement." *International Journal of Thermal Sciences* 109 (2016): 1-9. https://doi.org/10.1016/j.ijthermalsci.2016.05.025

[51] Hilo, Ali Kareem, Antonio Acosta Iborra, Mohammed Thariq Hameed Sultan, and Mohd Faisal Abdul Hamid. "Experimental study of nanofluids flow and heat transfer over a backward-facing step channel." *Powder technology* 372 (2020): 497-505. https://doi.org/10.1016/j.powtec.2020.06.013

[52] Nfawa, Sadeq Rashid, Abd Rahim Abu Talib, Siti Ujila Masuri, Adi Azriff Basri, and Hasril Hasini. "Heat transfer enhancement in a corrugated-trapezoidal channel using winglet vortex generators." *CFD Letters* 11, no. 10 (2019): 69-80.

[53] Krishna, Ram, Niranjan Kumar, and Pankaj Kumar Gupta. "CFD investigation of pressure drop reduction in hydrotransport of multisized zinc tailings slurry through horizontal pipes." *International Journal of Hydrogen Energy* 48, no. 43 (2023): 16435-16444. https://doi.org/10.1016/j.ijhydene.2023.01.116

[54] Firoozeh, Saeed Takht, Nader Pourmahmoud, and Morteza Khalilian. "Two-tube heat exchanger with variable groove angle on the inner pipe surface: Experimental study." *Applied Thermal Engineering* 234 (2023): 121274. https://doi.org/10.1016/j.applthermaleng.2023.121274

[55] Ali, Munazid, Ariana I. Made, and Utama I. Ketut Aria Pria. "CFD Analysis on the Development of Pre-Duct Shape to Improve Propeller Performance." *CFD Letters* 16, no. 2 (2024): 118-132. https://doi.org/10.37934/cfdl.16.2.118132

[56] Ghobadi, Mehdi, and Yuri Stephan Muzychka. "A review of heat transfer and pressure drop correlations for laminar flow in curved circular ducts." *Heat Transfer Engineering* 37, no. 10 (2016): 815-839. https://doi.org/10.1080/01457632.2015.1089735

[57] Azhari, Abdullah A., Ahmad H. Milyani, Nidal H. Abu-Hamdeh, and Amira M. Hussin. "Thermal improvement of heat exchanger with involve of swirl flow device utilizing nanomaterial." *Case Studies in Thermal Engineering* 44 (2023): 102793. https://doi.org/10.1016/j.csite.2023.102793